ENHANCEMENT OF THE PHOTOCATALYTIC PROPERTIES OF TITANIA NANOPARTICLES BY DOPING LANTHANIDE IONS

ZEINHOM M. EL-BAHY†*, ADEL A. ISMAIL‡, REDA M. MOHAMED‡

† *Department of Chemistry, Faculty of Science, Al-Azhar University, Nasr City 11884, Cairo, Egypt*
‡ *Central Metallurgical R and D Institute, CMRDI, P.O. Box 87 Helwan, Cairo, Egypt*

Abstract

Lanthanide ions (La^{3+}, Nd^{3+}, Sm^{3+}, Eu^{3+}, Gd^{3+}, and Yb^{3+})- doped TiO$_2$ nanoparticles were successfully synthesized by sol-gel method to enhance the photocatalytic activity of the developed materials. The structural features of TiO$_2$ and lanthanide ions–doped TiO$_2$ fired at 550ºC were investigated by XRD, UV-diffuse reflectance, and nitrogen adsorption measurements. The effect of lanthanide ions-doped TiO$_2$ on the photoactivity was evaluated by the degradation of direct blue dye (DB 53) as a probe reaction. Our findings indicated that XRD data verified the formation of typical characteristic anatase reflections without any separate dopant-related peaks in all the prepared lanthanide ion-doped TiO$_2$ nanoparticles. The particle size of lanthanide ions-doped TiO$_2$ nanoparticles was smaller than pure TiO$_2$ indicating the improvement of its surface morphology. The results indicated that Gd^{3+}-TiO$_2$ has the lowest bandgap and particle size and the highest surface area and pore volume (Vp) as well. The photocatalytic behavior of lanthanide ions-doped TiO$_2$ was tested for oxidation of DB 53 in the presence of UV light at λ = 365 nm. It was found that Gd^{3+}-TiO$_2$ is the most effective catalyst in the photocatalytic activity studies. That might be due to its special characteristics of particle size, surface texture and bandgap properties. Our results should provide a significant contribution to the understanding of the chemistry of lanthanide ion-doped TiO$_2$ systems. Details of the synthesis procedure and results of the characterization studies of the produced lanthanide ions-TiO$_2$ are presented in this paper.

Introduction

During the recent decades, the photocatalytic application using semiconductors has been received much attention to solve the environmental problems [1-4]. TiO$_2$ has turned out to be the semiconductor with the highest photocatalytic activity, being non-toxic, stable in aqueous solution and relatively inexpensive [5]. The photocatalytic property of TiO$_2$ is due to its wide bandgap and long lifetime of photo generated holes and electrons. The high degree of recombination of the photo generated electrons and holes are a major limiting factor controlling its

photocatalytic efficiency and impeding the practical application of these techniques in the degradation of contaminants in water and air. Thus, a major challenge in heterogeneous photocatalysis is the need to increase the charge separation efficiency of the photocatalysts [6].

Although TiO_2 is the most widely used photocatalyst, attention has been paid to metal ions-doped titania and testing their efficiency to replace pure TiO_2 and enhance the photocatalytic conversions. In order to decrease the bandgap of parent titania photocatalyst (Eg = 3.2 ev), slow down the recombination rate of the e^-/h^+ pairs and enhance interfacial charge-transfer efficiency, the properties of TiO_2 have been modified by selective surface treatments such as surface chelation, surface derivatization, platinization, and by selective metal ions doping TiO_2 [7]. Coupled semiconductor photocatalysts exhibited a very high photocatalytic activity for both gas and liquid phase reactions. Researchers had much interest in coupling two semiconductor particles with different bandgap widths such as TiO_2-CdS, TiO_2-WO_3, TiO_2-SnO_2 [8], TiO_2 –MoO_3 [9] TiO_2-SiO_2 [10] and TiO_2–Fe_2O_3 [11,12].

Lanthanide ions are known for their ability to form complexes with various Lewis bases e.g. acids, amines, aldehydes, alcohols, thiols, …..etc) in the interaction of these functional groups with the f-orbitals of the lanthanides. Particularly, RE-modified TiO_2 nanoparticles become of current importance for maximizing the efficiency of photocatalytic reactions, increase the stability of anatase phase and prevent the segregation of TiO_2 [13-16]. Thus, incorporation of lanthanide ions into a TiO_2 matrix could provide a means to concentrate on the organic pollutant at the semiconductor surface and consequently enhance the photoactivity of titania [16-19]. It was reported in literature that the optimum level of RE-doping is 1-2% to hinder the crystal growth of titania during calcination [15]. Although doping of lanthanide ions into TiO_2 attracted some attentions [20-25], such works are little so far.

Investigating of the effect of the addition of lanthanide ions (1 wt%) doped TiO_2 is a crucial task for collecting more information about lanthanide ions-TiO_2 systems and its impact on the catalytic activity for the photodegradation of DB 53. The primary deriving force in this work is to prepare lanthanide ions-doped TiO_2 by sol-gel method and study its impact on the structure, bandgap, surface texture of TiO_2 nanoparticles. Moreover, the removal of one of the organic pollutants (namely Direct Blue 53 dye) was investigated as a pattern of organic pollutant to evaluate the relative photocatalytic activity of the prepared photocatalyst samples.

Experimental

Materials:

Titanium isopropoxide, Ytterbium (III) nitrate tetrahydrate, Neodymium nitrate hexahydrate, Samarium nitrate hexahydrate, Europium acetate tetrahydrate, Gadolinium (III) oxide and Lanthanum nitrate hexahydrate were used as precursors in the sol-gel preparations. Distilled water was used and all other chemicals were analytical grade. Direct Blue 53 (DB53), (molecular formula = $C_{34}H_{24}N_6Na_4O_{14}S_4$, molecular weight = 960.81), Scheme 1, was used.

The parent TiO_2 and lanthanide ions-doped TiO_2 nanoparticles were prepared by sol-gel technique. The sol corresponds to the overall molar ratio of $Ti(C_4H_9O_4)$: C_2H_5OH : H_2O : HNO_3 = 1 : 20: 4: 0.001. $Ti(C_4H_9O_4)$ was first dissolved in ethanol medium to form titania sol; the lanthanide salts were dissolved into stoichiometric amount of water and nitric acid and then added drop wise into the titania sol through stirring for 30 minutes at room temperature. The prepared sol was left to stand for the formation of gel and dried at 120ºC. Finally, the obtained gel was calcined at 550°C for 5 hrs to keep the lanthanide ions-TiO_2 in the anatase phase that has high photoactive sites. The atomic ratio of Ti^{4+}: lanthanide ions was kept as 99: 1 for all lanthanide ions -doped nanoparticles which still maintained a single anatase modification even at high temperature ≤ 900°C [14].
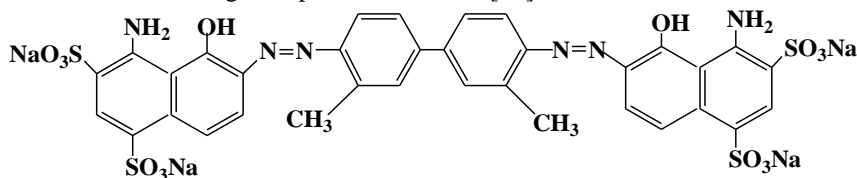
Scheme 1. Structure of Direct Blue 53 dye

Methods:

X-ray powder diffraction (XRD) patterns were taken at room temperature using a model Bruker axs, D8 Advance. Average crystallize size (D) of the obtained powders were calculated by x-ray line broadening technique performed on the direction of lattice using computer software based on the so-called Hall-equation-Scherer's formula $D = 0.89\lambda/\beta\cos\theta$ [26], where D is the crystallite size, λ represents the x-ray wavelength, θ is the Bragg's angle and β is the pure full width of the fraction line at half of the maximum capacity. The surface texture characteristics

obtained from nitrogen adsorption isotherms were measured at −196ºC using a conventional volumetric apparatus. The specific surface area was obtained using the BET method. The samples were thermally degassed at 300ºC prior to the adsorption measurements. The micropore volume and the external surface area were obtained from the *t*-plot. Bandgap *(E$_g$)* of the samples were determined by using JASCO (V 570) software based on the so-called direct transition formula αhγ = constant (hγ − Eg)^n [27], where α is extinction coefficient [cm^{-1}]; γ is wavenumber [cm^{-1}]; h is the blank constant.

The photodegradation experiments were carried out by dissolving pure DB53 dye in nanopure water at the desired concentration (dye conc. = 100 ppm, pH ≈ 7; unless otherwise stated). The catalyst loading was 0.075 g/300 ml (unless otherwise stated) and appropriate quantities of the suspensions were then transferred to the cells used for irradiation experiments. Typically, the mixture (catalyst + dye) was stirred continuously for 30 min in dark prior to illumination with UV Lamp to ensure attaining complete adsorption and to monitor the change in dye concentration due to adsorption. The cell was exposed to the UV lamp (150 W) for 60 min at 25 °C. In the continuous recirculation mode experiments, aliquots (5 ml) were retrieved from the reservoir at certain time intervals and analyzed after filtering through millipore filter (0.2 mm). The concentration of the unreacted DB 53 dye was analyzed with UV JASCO (V 570). The removal % of DB 53 dye was measured by applying the following equation.

$$Removal \% = \frac{(C_o - C)}{C_o} x100$$

Where *C$_o$* and *C* are the initial concentration of DB 53 and its remaining concentration in solution after reaction.

Results and Discussions

Evaluation and characterization of synthesized material

The crystalline phase of each parent TiO$_2$ and lanthanide ions-doped TiO$_2$ nanoparticles prepared by sol-gel was determined by powder XRD and the phase changes are shown in Fig. 1. In parent titania and all lanthanide ions -doped TiO$_2$ photocatalysts, the figure presents a group of lines at 2θ values of 25.2, 37.5, 47.7, 53.3, 54.7 and 62º which are attributed to anatase phase [PDF # 71-1169]. No diffraction peaks of lanthanide oxides in the patterns of lanthanide ions-TiO$_2$ doped samples were observed. This is probably due to the low lanthanide ions doping content (*ca.*1%) and the data may also imply that, the lanthanide oxides are well
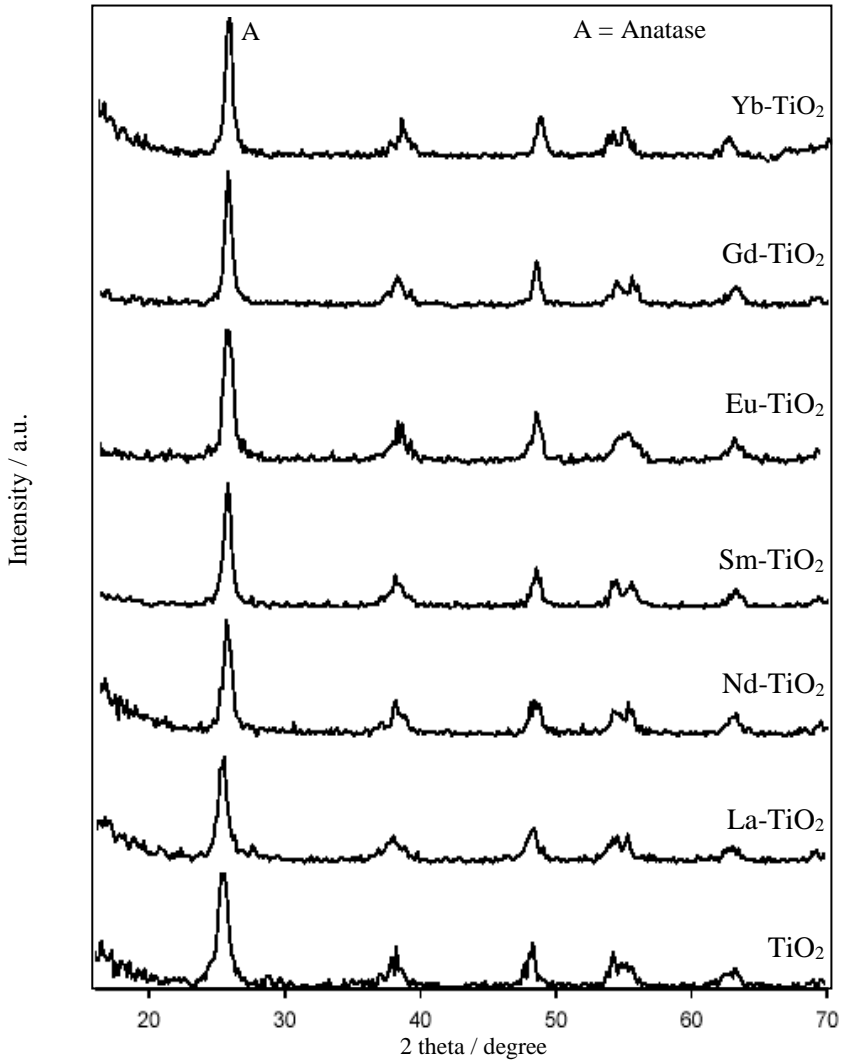
Fig.1. XRD patterns of parent TiO₂ and RE-TiO₂ nanoparticles

dispersed within the TiO_2 phase. The XRD data revealed that all the studied lanthanide ions inhibit the phase transformation from anatase to rutile during calcinations even at high temperatures (*ca.* 550ºC) while in other works, the anatase phase started to convert into rutile before 500ºC [28]. The crystallite size, calculated from Scherrer equation (D) of pure TiO_2 and lanthanide ions-doped TiO_2 is listed in Table 1. The X-ray diffraction peak of crystal plane (101) at $2\theta = 25.2º$ was

selected to determine the D value. The crystallite size value is ranging from 20.3 to 29.5 nm; the lanthanide ion-doped TiO_2 is lower carystallite size than TiO_2. This reduction in crystallite size is proposed due to segregation of the dopant cations at the grain boundary which inhibits the grain growth by restricting direct contact of grains [15]. The ionic radii of Ti^{4+} is much smaller than those of lanthanide ions (*r* for Ti^{4+} = 0.68 Å, whereas *r* for La^{3+}, Nd^{3+}, Sm^{3+}, Eu^{3+}, Gd^{3+} and Yb^{3+} = 1.032, 0.983, 0.958, 0.947, 0.938 and 0.868 Å, respectively [29]. From forgoing data Ti^{4+} may substitute for lanthanide oxides in the lattice of rare earth oxides to form tetrahedral Ti sites. The interaction between the different tetrahedral Ti atoms or between the tetrahedral Ti and octahedral Ti inhibits the phase transformation to rutile [17].

Table   1:   Effect of type of lanthanides ions on Crystallite size, band gab and photoactivity of lanthanides oxides- doped TiO_2

Sample	Crystallite size, nm	Bandgap eV	Photoactivity, %
TiO_2	29.5	3.5	86
La-TiO_2	22.1	3.35	89.9
Nd-TiO_2	22.6	3.48	86.4
Sm-TiO_2	21.9	3.45	87.3
Eu-TiO_2	23.4	3.34	90
Gd-TiO_2	20.3	3.27	91.5
Yb-TiO_2	28.9	3.36	89.8

The bandgap plays a critical role in deciding the photocatalytic activity of photocatalysts for the reason that it participates in determining the e-/h+ recombination rate. It was estimated by the diffuse reflectance absorption spectrum and summarized in Table 1. It was clearly seen that, doping with lanthanides ions has a great advantage specifically in the decrease in bandgap of TiO_2, which has a pronounced effect of the semiconduction properties of the prepared nanoparticles. It has been established that anatase crystallites of this size exhibit bulk physical properties when the particle diameters are larger than 5 nm [30,31]. The obtained nitrogen adsorption-desorption isotherms for the parent TiO_2 and that of lanthanide ions-doped TiO_2 samples are typical of type II of Brunauer's classification with a small hystresis loop, the isotherm of Gd-TiO_2, as an example, is shown in Fig 2. The

hystresis loop indicates that, the samples have porosity. The surface area, texture parameters calculated from the *t*-plot were estimated by the low-temperature nitrogen adsorption at relative pressures (P/P^0) in the range of 0.05–0.9 and are given in Table 2. An increase in the adsorption capacity of the TiO_2 was observed after introducing lanthanide ions. The surface area of Gd^{3+}-TiO_2 was changed from 223 to 390 m^2/g ($\approx$ 75% increase of surface area compared to the parent TiO_2). It is worth to mention that, the S_{BET} values of the prepared photocatalysts are relatively higher than that of other analogues samples as mentioned in literature [32], Table 2. Furthermore, the total pore volume of lanthanide oxides-TiO_2 was twice that of TiO_2. Since the TiO_2 (anatase) structure is not affected by doping with lanthanide ions as revealed by XRD, the increase of surface area and mesopore volume was observed for the lanthanide ions-doped TiO_2.

Further data assessment reveals that, the values of S_{BET} and S_t are generally close in most samples indicating the presence of mesopores. The values of external surface area (S_{ext}) of the samples are very small which verifies the porous nature of these solids. The values of S_{meso} are high compared to that of S_{micro} implying that the main surface is mesoporous solid as represented by the isotherm. The surface texture data will be correlated with the catalytic activity as will be mentioned later on.
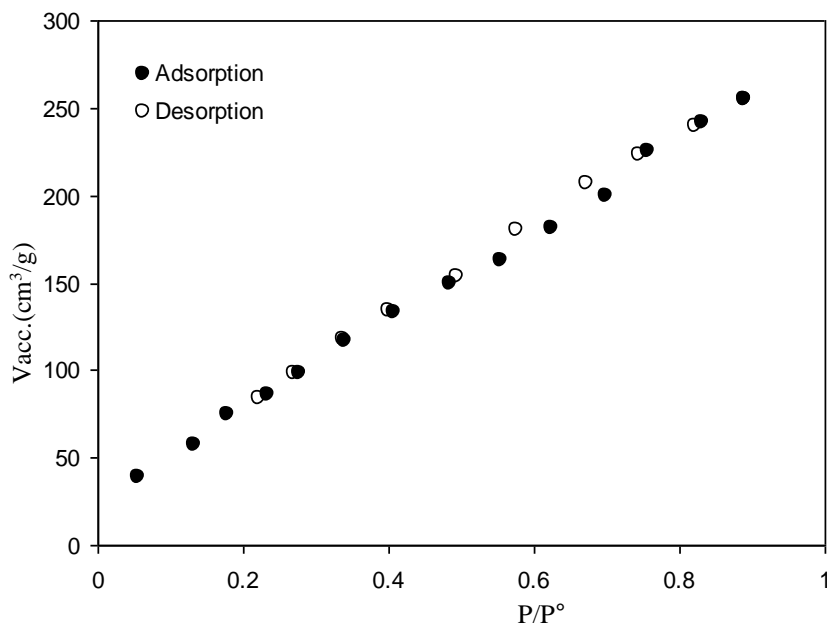

Fig. 2. Nitrogen adsorption-desorption isotherms of Gd-TiO₂

ZEINHOM M. EL-BAHY., *et al.,*

Table 2. Textural parameters* of the lanthanides doped TiO₂ nanoparticles

Sample	S_{BET} (m²/g)	S_t (m²/g)	$S_{(mic)}$ (m²/g)	$S_{(meso)}$ (m²/g)	$S_{(ext)}$ (m²/g)	V_p (cm³/g)	$V_{(mic)}$ (cm³/g)	$V_{(mes)}$ (cm³/g)	r (Å)
TiO_2	223	363	21	201	23	0.193	0.184	0.009	21.67
$La\text{-}TiO_2$	349	360	63	285	34	0.392	0.313	0.079	28.14
$Nd\text{-}TiO_2$	312	244	24	287	12	0.224	0.194	0.029	17.97
$Sm\text{-}TiO_2$	341	368	80	260	24.1	0.413	0.352	0.060	30.28
$Eu\text{-}TiO_2$	367	368	66	300	36	0.406	0.321	0.085	27.71
$Gd\text{-}TiO_2$	390	416	81	308	30	0.425	0.35	0.071	27.27
$Yb\text{-}TiO_2$	331	337	57	273	26	0.355	0.297	0.058	26.87
TiO_2 [a]	173								
$Eu\text{-}TiO_2$ [a]	176								

*(S_{BET}) BET-Surface area, (S_t) surface area derived from $V_{l\text{-}t}$ plots,(S_{mic}) surface area of micropores , (S_{mes}) surface area of micropores, (S_{ext}) external surface area
(V_p) total pore volume, (V_{mic}) pore volume of micropores, (V_{mes}) pore volume of mesopores and (r) mean pore radius.
a- Data from reference [32].

Photocatalytic activity studies

The photodegradation of DB53 dye was used as a probe reaction to test the photocatalytic activity of the prepared nanoparticles. Fig. 3 shows the effect of lanthanide oxides-doped titania nanoparticles on photocatalytic degradation of DB53 dye after 30 min at 25°C using 100 ppm of the BD53 at pH 7.7 and 0.25 gm catalyst/1000 ml dye solution.
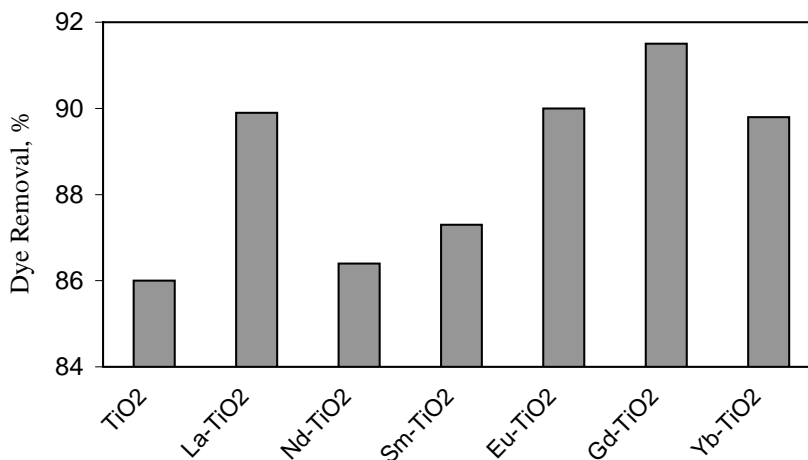

Fig.3. Effect of lanthanide ion- doped TiO₂ on the photoactivity

The data presents that the photocatalytic activities of the lanthanide ions-doped titania nanoparticles is higher than that of parent TiO_2. Knowing that, the pure lanthanide oxides don't have photocatalytic oxidation properties, such variation in activity must be due to the differences in interaction between lanthanide ions oxides and TiO_2. That led to several modifications in physical properties such as bandgap, particle size and surface texture. The photocatalytic activity of titania generally increased with the addition of lanthanide ions promoters. From the foregoing data, it was clear that the photocatalytic activity of Gd-TiO_2 was the optimum.

In La^{3+}, Nd^{3+}, Sm^{3+}, Eu^{3+}, Gd^{3+} and Yb^{3+}-TiO_2 mixtures, as mentioned before, Ti^{4+} may replace the lanthanide oxides with a trivalent oxidation state and creates a charge imbalance. The charge imbalance must be satiated; therefore more hydroxide ions would be adsorbed on the surface for charge balance. These hydroxide ions on the surface can accept holes generated by UV illumination to form hydroxyl radicals, which oxidize adsorbed molecules and therefore decrease the e^-/h^+ recombination rate. Fig. 4 demonstrates the correlation between the photoactivity and the physical properties such as bandgap, surface area and pore volume.
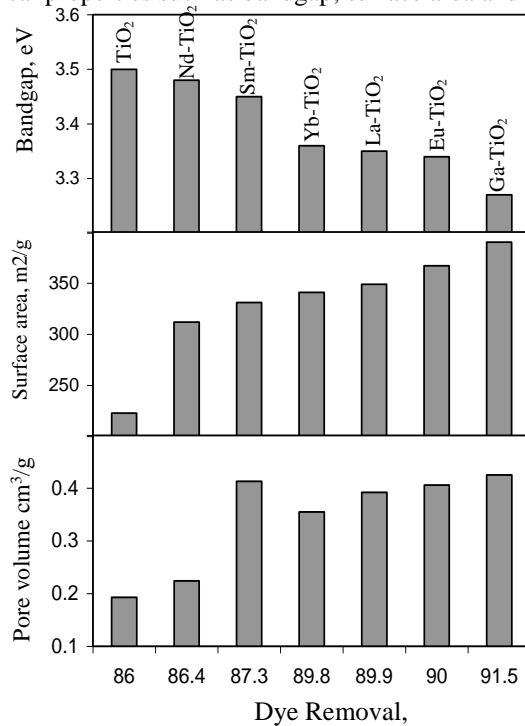

Fig.4. Effect of physical parameters of the materials on their photoactivity

It is clear that, the photocatalytic activity of Gd-TiO$_2$ was the highest due to it has high surface area and pore volume and low bandgap. Fig. 4 showed the good correlation between the bandgap, surface area and pore volume with the photocatalytic activity where the activity was gradually increased with the decrease of bandgap and the increase of the surface area and pore volume.

The results show that the photocatalytic activities of lanthanide ions doped titania nanoparticles increased with decreasing the bandgap. This is due to decrease energy to exit electron from conduction band to valance band. The high activity of Gd^{3+}-TiO$_2$ dopants may also be related to its half filled (*t*) electronic configuration.
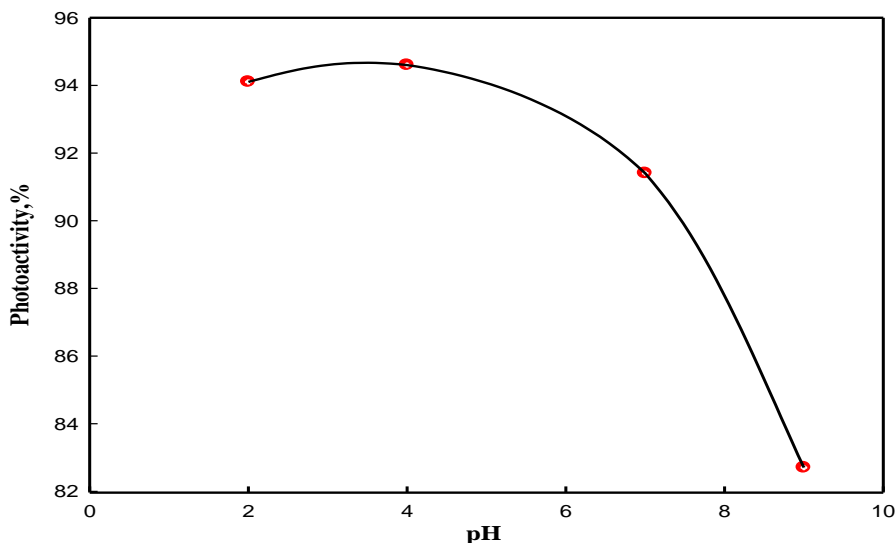

Fig. 5. Effect of pH on the photoactivity

The variation of pH value on the photoactivity (lanthanide oxides-doped TiO$_2$) on the photodegradation of DB53 dye was extensively studied. Fig. 5 shows the effect of pH of dye solution on its photocatalytic oxidation over Gd-TiO$_2$ after 30 min of reaction using the previous stated reaction conditions. The findings show that the increase of the dye solution pH from 2 to 9 decreases the photocatalytic activity from 94.1 to 82.7, respectively. Such trend may be due to the fact that, DB53 dye has negative charge, whereas lanthanide ions-TiO$_2$ has positive charge in acidic medium. Consequently, the increase in pH value tended to change the charge on

lanthanide ions-TiO_2 to negative charge and in turn, the photoactivity decreased due to the repulsion between lanthanide oxides-TiO_2 and anionic dye [33]. In addition, the increase of pH may increase the rate of e^-/h^+ recombination rate and thus decreases the catalytic activity. Therefore, the optimum pH value for the photo degradation of DB53 dye is $\approx$ 4 at which photocatalytic oxidation is being maximum.

About 60 % of DB53 dye (100 ppm) was photodegraded on the surface of Gd-TiO_2 after 5 min as shown in Fig 6. The remained dye was completely oxidized within 40 min. Such data reveals the relative high activity of the prepared catalysts which enables the complete degradation of the pollutant in such short time.

Regarding the loading catalyst, the results show that the increment of catalyst loading from 0.1 to 0.5 g/l increased the photoactivity from 75 to 100 % respectively, Fig. 7, and then the activity became steady above 0.3 g/l loading catalyst. With increasing the weight above 0.4 g/l, the activity decreased. These results are in good agreement with the data reported in literature [34,35]. The reasons for this decrease in degradation rate were aggregation of lanthanide oxides-TiO_2 particles at high concentration causing a decrease in the number of surface active sites and increase the opacity and light scattering of lanthanide oxides-TiO_2 particles at high
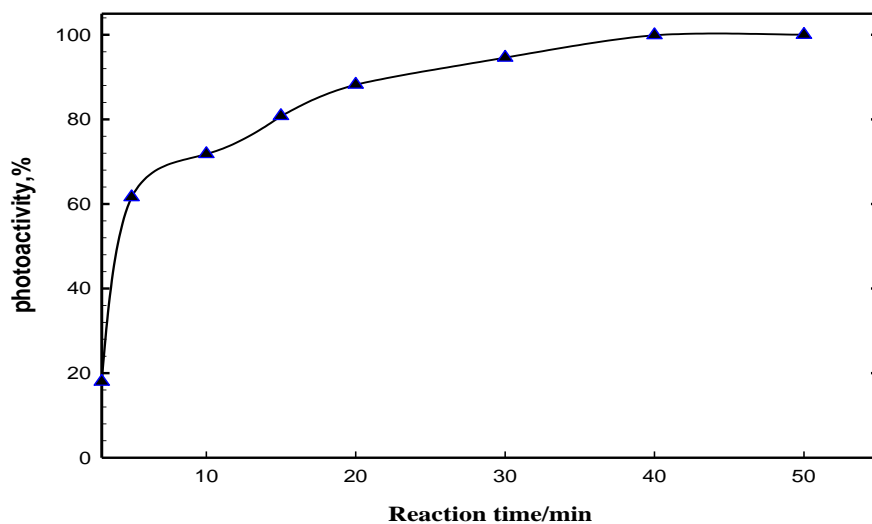

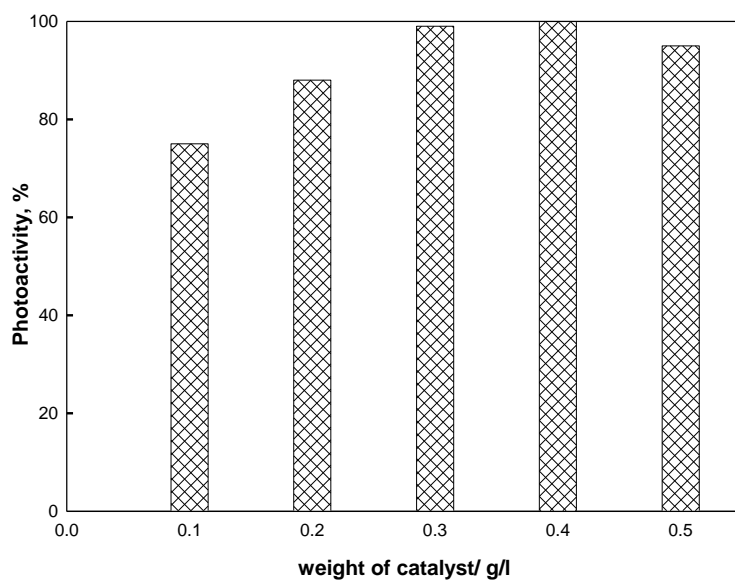**Fig.6. Effect of reaction time on the photoactivity**

ZEINHOM M. EL-BAHY., *et al.,*

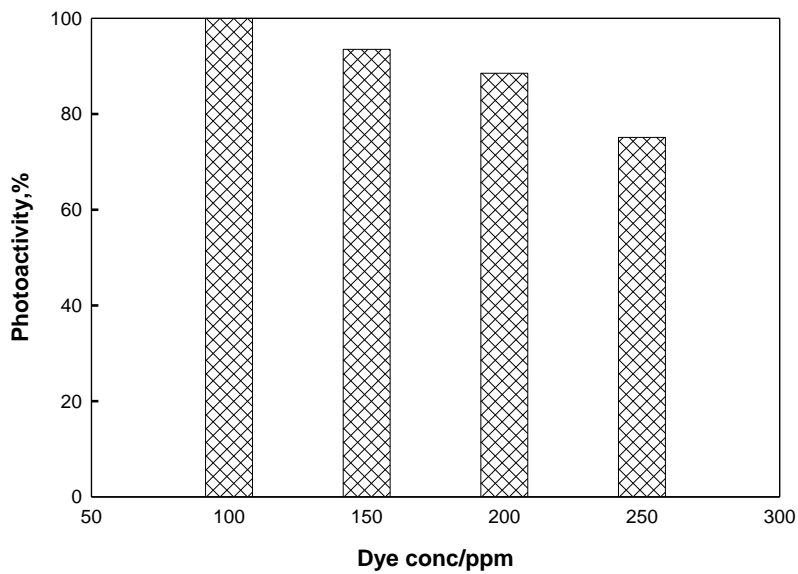**Fig. 7. Effect of photocatalyst weight on its photoactivity**

Fig. 8. Effect of initial dye concentration on photoacaivity

concentration. This tends to decrease the passage of irradiation through the sample [36]. Therefore, the best catalyst loading is 0.3 g/l.

The effect of the initial dye concentration on the photocatalytic oxidation of DB53 dye was also studied and the obtained data is given in Fig. 8. The results show that the increment of initial dye concentration from 100 to 250 ppm led to a decrease in the photocatalytic degradation of DB53 from $\approx$ 100 to 75.1 % respectively. The rate of degradation relates to the formation of hydroxyl radicals, which is the critical species in the degradation process. Hence an explanation to this behavior is that the higher the initial concentration, the higher adsorbed organic substances on the surface of lanthanide ions -TiO$_2$. In the same time the intensity of light and illumination are constant, so the path length of photons entering the solution decreases and in low concentration, the reverse effect is observed and consequently the OH$^{\bullet}$ radicals formed on the surface of lanthanide ions-TiO$_2$ nanoparticles decrease. With decreasing the number of OH$^{\bullet}$ radicals attacking the surface, the relative OH number attaching the compound decreases and thus the photo degradation efficiency decreases [35].

Conclusions

The sol–gel method is useful for the preparation of nanostructured lanthanide ions -TiO$_2$ with high photocatalytic activity, high surface area and desirable pore structures. A series of Nd, Sm, Eu, Gd, Yb and La homogenously doped nanocrystalline TiO$_2$ has been successfully synthesized by sol gel method. The type of dopant lanthanide ion showed significant effect on the texture structure, bandgap and particle size. These physical changes affected on the efficiency of the photodegradation of DB53 dye. The photoactivity is well correlated with the bandgap, surface area and pore volume. In addition, the differences in photoactivity are due to the change in the amount of surface hydroxyl groups resulting from the interaction between the rare earth oxides and TiO$_2$. The Gd-TiO$_2$ nanoparticles presented the highest photoactivity due to its high surface area, large pore volume, small particle size and small bandgap.

References

1. P.C. CALZA et al., Adv. Mater. 17 (2005) 2467.

2. H. KISCH , W. MACYK, Chem Phys Chem. 3 (2002) 399.

3. A. P. DAVIS, D. L. GREEN, Environ. Sci. Technol. 33 (1999) 609.

4. H. CHOI, A.C. SOFRANKO, D.D. DIONYSIOU, Adv. Funct. Mater. 16 (2006) 1067.

5. A.P. HONG, D.W. BAHNEMANN, M.R. HOFFMANN, J. Phys. Chem. 91 (1987) 2109.

6. H. HIDAKA, Y. ASAI, J. ZHAO, K. NOHARA, E. PELIZZETTI, N. SERPONE, J. Phys. Chem. 99 (1995) 8244.

7. L. KRUCZYNSKI, H.D. GESSER, C.W.TURNER, E.A.SPEER, Nature 291 (1981) 399.

8. N. SERPONE, P. MARUTHAMUTHU, E. PELIZZETTI, H. HIDAKA, J. Photochem Photobiol A 85 (1995) 247.

9. K.Y. SONG, M.K. PARK, Y.T. KWON, H.W. LEE, W.J. CHUNG, W.I. LEE, Chem. Mater. 13 (2001) 2349.

10. A.A. ISMAIL, I.A. IBRAHIM, R.M. MOHAMED, H. EL-SHALL, J. Photochem Photobiol. A 63 (2004) 445.

11. B. PAL, T. HATA, K. GOTO, G. NOGAMI, J. Mol. Catal. A 169 (2001) 147.

12. A.A. ISMAIL, Appl. Catal. B 58 (2005) 115.

13. Y. WANG, H. CHENG, L. ZHANG, Y. HAO, J. Ma, B. Xu, W. Li, J. Mol. Catal. A 151 (2000) 205.

14. Y. ZHANG, H. ZHANG, Y. XU, Y. WANG, J. Solid State Chem. 177 (2004) 3490.

15. Y. ZHANG, H. XU, H. ZHANG , Y. WANG, J. Photochem Photobiol A 170 (2005) 279.

16. K.T. RANJIT, I. WILLNER, S.H. BOSSMANN, A.M. BRAUN, Environ. Sci. Technol. 35 (2001) 1544.

17. J. Lin, J.C. Yu, J. photochem. Photobiol.A 116 (1998) 63.

18. D.W. HWANG, J.S. LEE, W. LI, S.H. OH, J. Phys. Chem. B 107 (2003) 4963.

19. Y.H. ZHANG, H.X. ZHANG, Y.X. XU, Y.G. WANG, J. Mater. Chem. 13 (2003) 2261.

20. J. LIN, J. YU, S.K. Lam, J. Catal. 183 (1999) 368.

21. R.GOPALAN, Y.S. lin, Ind. Eng. Chem. Res. 34 (1995) 1189.

22. G. BOSCHLOO, A. HAGFELDT, Chem. Phys. lett. 370 (2003) 381.

23. A. Xu, Y. GAO, H. LIU, J. Catal. 207 (2002) 151.

24. M.S.P. FRANCISO, V.R. MASTELARO, Chem. Mater. 14 (2002) 2514.

25. C.P. SIBU, K.S. RAJESH, P. MUKUNDAN, K.G.K. Warrier, Chem. Mater. 14 (2002) 2876.

26. P. KLUG, L.E. ALEXANDER "Direction procedures for polycrystalline and amorphous materials" Wiley, (1954).

27. P. TYAGI, A.G. VEDESHWAR, Bull. Mater. Sci., 34 (2001) 297.

28. K.Y. JUNG, S.B. PARK, J. Photochem. Photobiol. A Chem. 127 (1999) 117.

29. R.D. SHANNON, Acta Crystallogr. A 32 (1976) 751.

30. C. KORMANN, W.D. BAHNEMANN, R.M. HOFFMANN, J. Phys. Chem. 92 (1988) 5196.

31. S. MONTICONE, R. TUFEU, V.A. KANAEV, E. SCOLAN, C. SANCHEZ, Appl. Surf. Sci. 162-163 (2000) 565.

32. P. YANG, C. LU, N. HUA, Y. DU, Mater. Lett. 57 (2002) 794.

33. C.A. LE DUC, J.M. CAMPBELL, J.A. ROSSIN, Ind. Eng, Chem. Res. 35 (1996) 2473.

34. D. CHEN, AK. Ray, Water Res. 32 (1998) 3223.

35. A. MILLS, S. MORRIS, J. Photobiol A 71 (1993) 75.

36. A.P. TOOR, A. VERMA, C.K. JOTSHI, P.K. BAJPAI, V. Singh, Dyes and Pigments 68 (2006) 53.